Bioresponsive *pseudo*Glucosinolates (*ps*GSLs) release Isothiocyanates (ITCs) in the Presence of Nitroreductases

Claire C. Jimidar,[b],# Charity S. G. Ganskow,[a],# Mervic D. Kagho,[a],# Aishi Chakrabarti,[a],# Lorenz Wiese,[b] Michael Zollo,[c] Ulrike Beutling,[d] Mark Brönstrup,[d] Stephan A. Sieber,[c] Stephan M. Hacker,[e] and Philipp Klahn*[a],[b]

[a]   C. S. G. Ganskow, A. Chakrabarti, Dr. Mervic D. Kagho, Prof. Dr. P. Klahn*
       Department of Chemistry and Molecular Biology, Division of Organic and Medicinal Chemistry
       University of Gothenburg
       Natrium, Medicinaregatan 7B, 413 90 Gothenburg, Sweden
       E-mail: philipp.klahn@gu.se
[b]   C. C. Jimidar, L. Wiese, Prof. Dr. P. Klahn*
       Institute of Organic Chemistry
       Technische Universität Braunschweig
       Hagenring 30, 38106 Braunschweig, Germany
[c]   M. Zollo, Prof. Dr. S. A. Sieber
       Center for Functional Protein Assemblies
       Technische Universität München
       Ernst-Otto-Fischer-Straße 8, 85748 Garching, Germany,
[d]   U. Beutling, Prof. Dr. M. Brönstrup
       Department for Chemical Biology
       Helmholtz Center for Infection Research
       Inhoffenstraße 7, 38124 Braunschweig, Germany
[e]   Dr. S. M. Hacker
       Department of Molecular Physiology, Leiden Institute of Chemistry
       Leiden University
       Einsteinweg 55, 2333 CC Leiden, The Netherlands

#   Authors contributed equally.

       Supporting information for this article is available.

Abstract: Glucosinolates (GSLs) are secondary metabolites produced as part of an herbivore defence system in plants of the order *Brassicales*. GSLs release isothiocyanates (ITCs) upon activation by the myrosinase. Beyond their herbivore feeding deterrent properties, these ITCs have multiple interesting bioactivities. However, their release is limited by the presence of myrosinase. Here, we report the concept of *pseudo*glucosinolates (*ps*GSLs) hijacking the natural release mechanism of GSLs for the release of ITCs and adapting it to nitroreductase as triggering enzymes. We provide the proof-of-concept for nitroreductase-responsive *ps*GSLs and demonstrate their potential for peptide labelling and ITC-prodrug approaches.

Introduction

Glucosinolates (GSLs) are secondary metabolites produced by plants of the order *Brassicales* such as broccoli, horse radish or white mustard as part of the GSL-myrosinase herbivore defence system.[1] Chemically GSLs are glycosidic thiohydroximate-*O*-sulfonates biogenetically derived from amino acids, which are stored in the tissue of the producing plants separated from the enzyme myrosinase, a thioglucosidase. Upon tissue damage the thioglycosidic bond of the GSLs is cleaved by the myrosinase releasing glucose and a thio-hydroximate-*O*-sulfonate aglycone,[2] which undergoes a subsequent thio-*Lossen* rearrangement forming isothiocyanates (ITCs) as active feeding deterrent agents

(Scheme 1A).[3,4] Beyond their feeding deterrent properties, ITCs have raised interest in recent years due to multiple interesting biological activities such as pollinator attraction,[5] antimicrobial activities[6,7] against bee-colony infecting fungi *Nosema ceranae*,[8,9] Methicillin-resistant *Staphylococcus aureus* (MRSA),[10] enterohemorrhagic *Escherichia coli* (EHEC)[11], *Pseudomonas aeruginosa* and related biofilms.[12] In addition, multiple specific bioactivities in mammalian cells have been reported, which might be summarized as neuroprotective, cardioprotective and chemoprotective.[13–18] Most of the biological activities of ITCs seem to be associated with their electrophilic reaction with biological nucleophiles.[11,19,20] GSLs as naturally occurring ITC-releasing molecules have therefore gained interest as intestinal formation of ITCs from GSLs is known to mediate the health beneficiary effects of *Brassicales* enriched dietary.[21–23]

Considering their interesting biological activities, it is not surprising that natural[17,24–28] as well as artificial GSLs have been synthesized including representatives bearing unnatural[17,28,29] or isotopically labeled[29–33] aglycones and glucose units as well as α-anomeric GSLs.[34,35] Furthermore, artificial GSLs have been designed to serve as myrosinase-responsive tool compounds in chemical biology. In 2018, *Tatibouët* and co-workers, reported the synthesis of mannoside-GSL conjugates, which allowed for myrosinase-triggered specific labelling of lectins[36] with released ITCs or synthesis of glycosylated proteins.[37] In 2019, we reported the synthesis and biochemical evaluation of **GSL-N₃** and **GSL-**

1

BODIPY (Scheme 1B), first examples of an azide bearing and artificial, fluorescent GSL, respectively, forming fluorescent **ITC-BODIPY** in the presence of myrosinase.[38] Independently, Tatibouët and co-workers, reported a similar approach for fluorescent GSLs and demonstrated their ability to serve as labelling probes for proteins.[39] Recently, we also have reported the synthesis of **GSL-DNSA** (Scheme 1B), which was utilized to image uptake through GTR receptors of *Arabidopsis thaliana*.[40] The major limitation for application of these probes in broader chemical biology context is the dependence on myrosinase, a thioglycosidase limited to the producing plants. Beyond that ITCs are hydrolysis sensitive electrophiles showing bad pharmacokinetic properties leaving their interesting biological activities unexploited.[1,41,42]

Within our attempts to design bio-responsive molecular entities[43–47] and explore the chemistry of artificial GSLs,[38,40,48] we aimed to translate the natural myrosinase-mediated release mechanism of ITCs from GSLs (Scheme 1A) towards artificial GSLs, which are bioresponsive towards enzymes other than the thioglucosidase myrosinase or even chemical triggers.

Therefore, we envisaged the design of artificial GSLs, in which the thioglycosidic trigger is substituted by a chemically masked *para*-aminobenzylthiol unit (Scheme 1C), which we named *pseudo*glucosinolates (*ps*GSLs).[48]
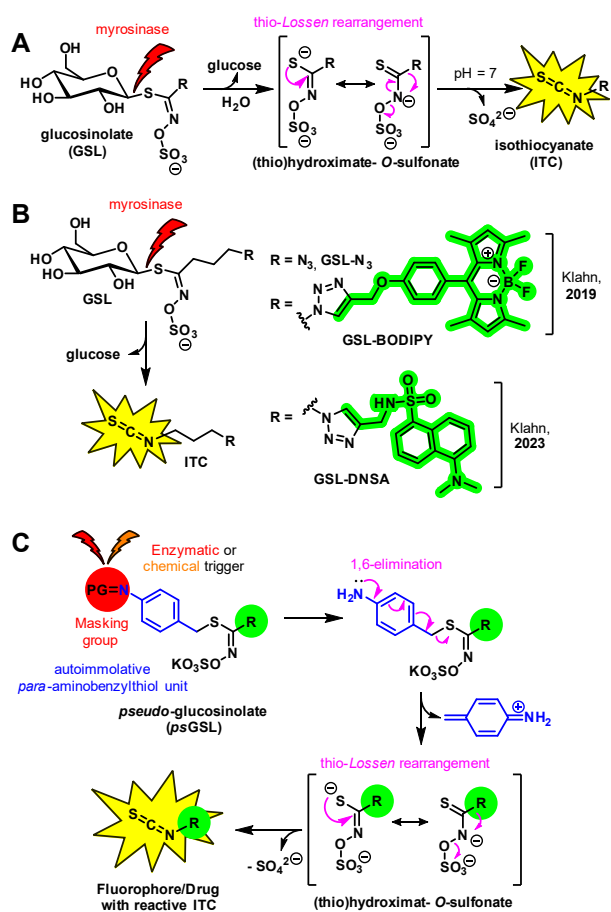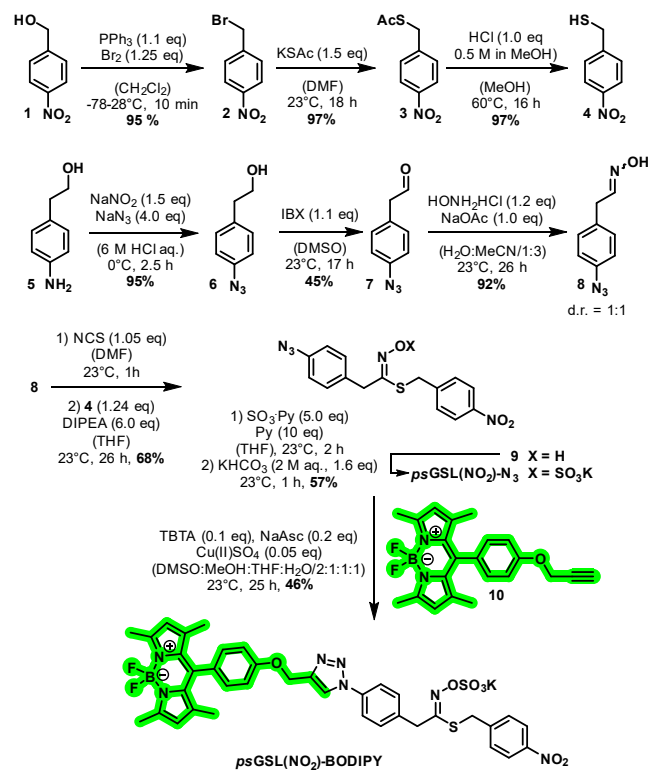
Upon enzymatic or chemical removal of the masking group *ps*GSLs were planned to mimic the natural release mechanism of ITCs from GSLs by undergoing first an auto-immolative 1,6-elimination of the free *para*-aminobenzylthiol moiety, leading to the thiohydroximate-*O*-sulfonate as intermediate, followed by the final formation of ITCs through a thio-*Lossen* rearrangement. Thus, *ps*GSLs could serve as prodrugs and tool compounds for the release of ITCs and their response might be adjusted to different enzymes and chemical triggers.

Results and Discussion

In order to prove our design concept of *ps*GSLs, we first aimed to synthesize potentially nitroreductaseresponsive *ps*GSLs **psGSL(NO₂)-N₃** and fluorescently labelled **psGSL(NO₂)-BODIPY** bearing a nitro-masked *para*-aminobenzylthiol unit as outlined in Scheme 2. For this purpose, commercially available *para*-nitrobenzylalcohol (**1**) was converted into thiol (**4**), which served as nitro-masked *para*-aminobenzylthiol building block. Initial *Appel*-type reaction at -78°C gave access to bromide **2**, which was subsequently substituted in the presence of potassium thioacetate to form the corresponding thioacetate **3**. While basic conditions for the cleavage of the thioacetate led to formation of the respective disulfide, acidic hydrolysis with methanolic HCl under an argon atmosphere provided the desired *para*-nitrobenzyl thiol (**4**) in 89% yield over 3 steps. As building block for the "*pseudo*-aglycone" we synthesized azido oxime **8** starting from the commercially available 2-(4-aminophenyl)ethanol **5**.

Scheme 1. A: GSL breakdown by myrosinase. **B:** Artificial, fluorescent and azide containing GSLs by *Klahn* and co-workers.[38,40] **C:** Design concept of novel *pseudo*glucosinolates (*ps*GSLs).[48] PG = protective group.

Scheme 2. Synthesis of *para*-nitrobenzylthiol (**4**) and potentially nitroreductase-responsive *ps*GSLs, namely **psGSL(NO₂)-N₃** and **psGSL(NO₂)-BODIPY**.

2
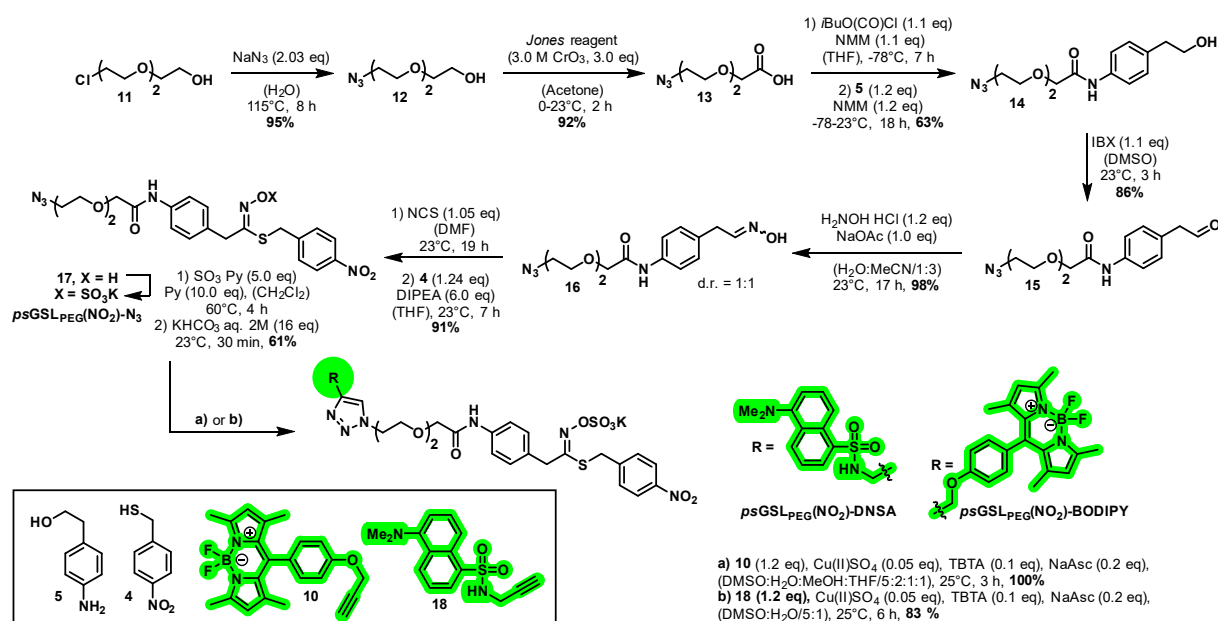
Scheme 3. Synthesis of *ps*GSL$_{PEG}$(NO$_2$)-N$_3$, *ps*GSL$_{PEG}$(NO$_2$)-BODIPY and *ps*GSL$_{PEG}$(NO$_2$)-DNSA.

Formation of the diazonium salt and subsequent substitution with sodium azide gave access to azido alcohol **6**, which was oxidized to the corresponding azido aldehyde **7** using IBX, and final conversion with hydroxylamine led to azido oxime **8** in 39% yield over 3 steps. Both building blocks, **8** and **4**, were coupled adapting the classical approach for the synthesis of GSLs.[24,28,38,49] First azido oxime **8** was converted *in situ* into its respective chloro oxime, and subsequently the substitution of the chloro atom with thiol **4** in the presence of *Hünig's* base facilitated formation of thiohydroximate **9** in 68% yield. Treatment of **9** with pyridine SO$_3$ complex and subsequent stirring with aqueous potassium bicarbonate solution gave access to *ps*GSL(NO$_2$)-N$_3$ in form of its potassium salt in 57% yield. Subsequent copper(I)-catalyzed azide-alkyne cycloaddition click reaction (CuAAC) with *meso*-substituted, alkyne-bearing BODIPY dye **10**[38] led to formation of the fluorescently labelled potential nitroreductase-responsive *ps*GSL, namely **psGSL(NO$_2$)-BODIPY**, in 46% yield. Unfortunately, although **psGSL(NO$_2$)-N$_3$** was water soluble, the *O*-sulfonate moiety was not sufficient to enable water solubility of **psGSL(NO$_2$)-BODIPY**, a requirement for the biochemical evaluation of the probe in the presence of nitroreductases. As the incorporation of water-soluble groups to the aromatic core of the *para*-aminobenzylthiol unit turned out to be synthetically challenging and flexibility for different fluorescent dyes was desired, we incorporated a PEG$_2$ motif into the core structure as outlined in Scheme 3. To this end, chloride **11** was converted to azide **12** in the presence of sodium azide at 115°C and subsequent *Jones* oxidation gave the ω-azido PEG$_2$ carboxylic acid **13**. *Iso*-butylchloro formate mediated amide coupling with aniline **5** gave alcohol **14** in 63% yield. Oxidation to the aldehyde **15** worked in 86% using IBX. Oxime formation, chlorination, coupling with *para*-nitrophenylthiol **4** and final installation of the *O*-sulfonate proceeded smoothly and gave **psGSL$_{PEG}$(NO$_2$)-N$_3$**. The CuAAC with the dansylamide **18** and BODIPY dye **10**, both bearing a terminal alkyne, provided access to **psGSL$_{PEG}$(NO$_2$)-DNSA** and **psGSL$_{PEG}$(NO$_2$)-BODIPY**, respectively, both showing decent water solubility. All synthesized *ps*GSLs showed decent chemical stability over months stored at -20°C or over weeks stored at 25°C being dissolved in either DMSO, HEPES or TRIS buffer (pH 7.4).

Next, we tested our hypothesis of ITC release from **psGSL$_{PEG}$(NO$_2$)-N$_3$** in the presence of nitroreductases by LC-MS analysis after incubation of the compounds with the commercially available nitroreductase (NTR) NfsB from *Escherichia coli* and required co-factors NADH and FMN in HEPES buffer (20 mM, pH 7.4) at 37°C. Coming from the enzymatic investigation of GSLs with the thioglucosidase myrosinase, which shows a relative slow conversion of their substrates,[38] we first incubated **psGSL$_{PEG}$(NO$_2$)-N$_3$** for 1 h at 37°C. As shown in Figure 1, **psGSL$_{PEG}$(NO$_2$)-N$_3$** (see Figure 1, A: structure, B1: R$_t$ 3.42 min and C1: mass 569 m/z for [M-K+2H]$^+$) is converted by NfsB and the formation of the corresponding ITC **19** (see Figure 1, A: structure, B2: R$_t$ = 4.10 min, and C3: mass 358 m/z for [M+Na]$^+$ and 336 m/z for [M+H]$^+$) is observed. In addition, we saw the formation of the corresponding hydroxylamine **21** (see Figure 1, A: structure, B2: R$_t$ = 2.63 min, and C2: mass 553 m/z for [M-K]$^-$). Furthermore, adding an excess of concentrated aqueous ammonia, both, ITC **19** and hydroxylamine **21** were rapidly converted into the corresponding thiourea **20** within minutes (see Figure 1, A: structure, B3: R$_t$ = 2.33 min, and C4: mass 375 m/z for [M+Na]$^+$, 353 m/z for [M+H]$^+$, 705 m/z for [2M+H]$^+$, and 727 m/z for [2M+Na]$^+$).

Next, we performed several control experiments (See Figure 1, D1-4) for the conversion of **psGSL$_{PEG}$(NO$_2$)-N$_3$** in the absence of the enzyme or cofactors NADH and FMN, with or without subsequent addition of an excess of 30% aqueous ammonia (10 μL ~ 157 μmol ~ 6284-fold excess compared to **psGSL$_{PEG}$(NO$_2$)-N$_3$**). In none of the control experiments we observed any conversion of **psGSL$_{PEG}$(NO$_2$)-N$_3$**; and in addition the compound was chemically stable under these highly basic conditions.
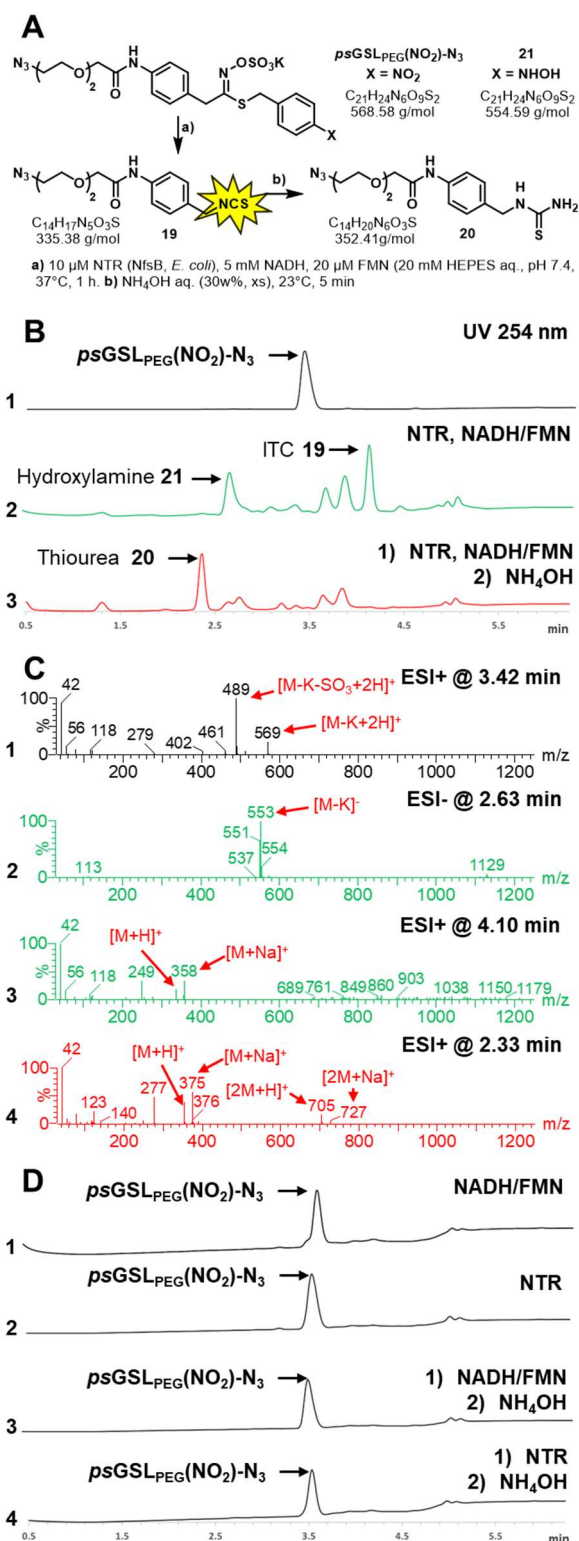
3

Figure 1. LC-MS analysis after incubation of *ps*GSL$_{PEG}$(NO$_2$)-N$_3$ with nitroreductase (NTR) NfsB from *E. coli* and subsequent derivatization with NH$_4$OH solution. **A:** Structures of *ps*GSL$_{PEG}$(NO$_2$)-N$_3$, ITC **19**, thiourea **20** and hydroxylamine **21**. **B:** UV chromatogram at 254 nm of (B1) pure *ps*GSL$_{PEG}$(NO$_2$)-N$_3$ (500 µM) in HEPES buffer (20 mM, pH 7.4), (B2) incubation of *ps*GSL$_{PEG}$(NO$_2$)-N$_3$ (500 µM) with NfsB (10 µM), NADH (5 mM) and FMN (20 µM) in HEPES buffer (20mM, pH 7.4) after 1 h at 37°C and (B3) B2 and addition of aqueous NH$_4$OH solution (30 w%, 10 µL). **C:** ESI+ or ESI- mass analysis at (C1) 3.42 min of B1, (C2 and C3) 4.10 min and 2.63 min of B2 and (C4) 2.33 min of B3. **D:** Control experiments following B2 or B3 in absence of NTR (D1 and D3) or the cofactors NADH and FMN (D2 and D3).
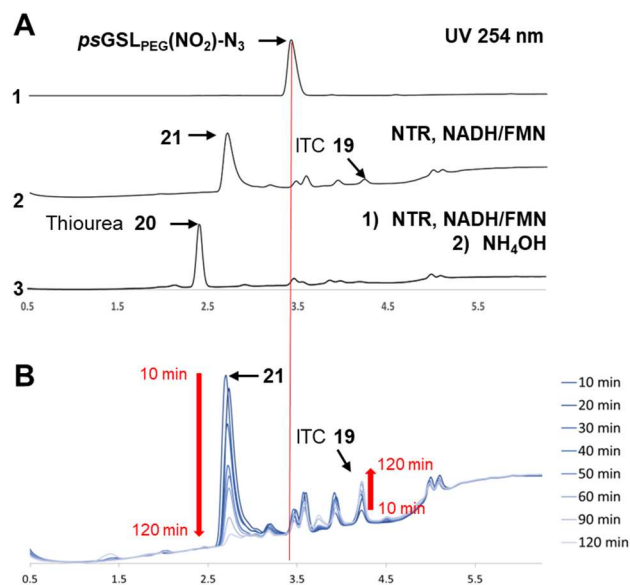

Figure 2. LC-MS analysis after incubation of *ps*GSL$_{PEG}$(NO$_2$)-N$_3$ with nitroreductase (NTR) NfsB from *E. coli* and subsequent derivatization with NH$_4$OH solution. **A:** UV chromatogram at 254 nm of (A1) pure *ps*GSL$_{PEG}$(NO$_2$)-N$_3$ (500 µM) in HEPES buffer (20 mM, pH 7.4), (A2) incubation of *ps*GSL$_{PEG}$(NO$_2$)-N$_3$ (500 µM) with NfsB (10 µM), NADH (5 mM) and FMN (20 µM) in HEPES buffer (20mM, pH 7.4) after 10 min at 37°C and (A3) A2 and addition of aqueous NH$_4$OH solution (30 w%, 5 µL) at 23°C. **B:** UV chromatogram at 254 nm of the conversion of *ps*GSL$_{PEG}$(NO$_2$)-N$_3$ (500 µM) in presence of NfsB (10 µM), NADH (5 mM) and FMN (20 µM) in HEPES buffer (20mM, pH 7.4) over the course of 2 h at 37°C (at t = 10, 20, 30, 40, 50, 60, 90, 120 min).

When monitoring the conversion of *ps*GSL$_{PEG}$(NO$_2$)-N$_3$ in the presence of NfsB and FMN/NADH after 10 min full conversion to the hydroxylamine **21** with only little conversion to the ITC **19** was observed in the LC-MS (See Figure 2, A2). Interestingly, both compounds were immediately converted into thiourea **20** when the reaction mixture was treated with an excess of aqueous ammonia (See Figure 2, A3) indicating a corresponding 1,6-elimination from the hydroxylamine **21** and addition of ammonia to the resulting ITC **19**. When the conversion of *ps*GSL$_{PEG}$(NO$_2$)-N$_3$ in the presence of NfsB and FMN/NADH was monitored over the course of 2 h, **21** was slowly consumed during the reaction under formation of the ITC **19** (Figure 2, B).

Considering that hydroxylamines are intrinsic intermediates in the 6-electron reduction of a nitro group to its corresponding amine by nitroreductases (Scheme 4), the observation of **21** as rapidly formed reduction product is reasonable. In addition, the nitroreductase NfsB from *E. coli* belongs to the oxygen insensitive nitroreductases of Type 1 performing two electron reductions[50,51] via a strongly substrate dependent ping-pong-bi-bi mechanism.[52,53] Meaning each 2-electron reduction product has to leave the active centre of the enzyme to allow the binding of a molecule NADH to reduce the prosthetic group FMN[50] again to FMNH$_2$. Afterwards, the release of NAD$^+$ allows binding of the next substrate in the active centre to be further reduced. Strongly depending on the affinity for the substrates, different product distributions are observed for *NsfB*.
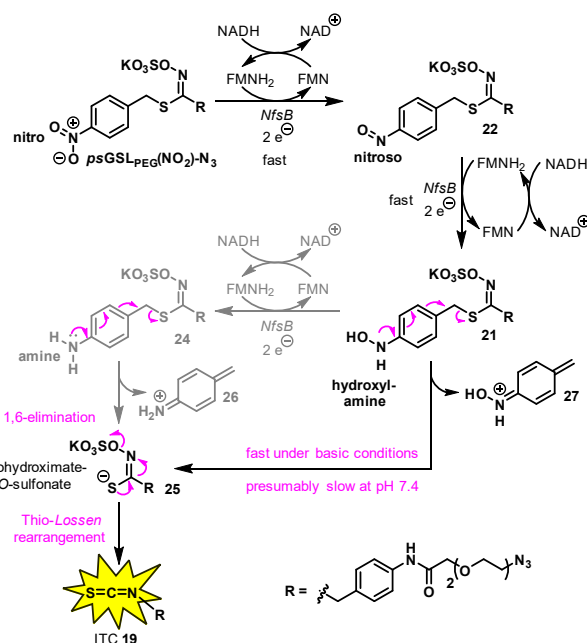
Indeed, NfsB is known to contribute to chloramphenicol resistance in Gram-negative bacteria by reduction of chloramphenicol to its corresponding inactive amino-chloramphenicol,[54,55] but likewise induces susceptibility of Gram-

4

negative bacteria towards nitrometronidazol by conversion into its hydroxylamine[55] involved in radical processes damaging the bacterial DNA.

In our current mechanistic understanding of the overall reaction, the initial reduction of **psGSL$_{PEG}$(NO$_2$)-N$_3$** to the corresponding nitroso compound **22** (only detected in traces, Scheme 4) and subsequently to the hydroxylamine **21** as major reduction product is fast. Whether the corresponding amine **24** (See, Scheme 4) is at all formed during the reaction is not clear. At least we do not detect **24** and it would be a relatively short-living intermediate anyway. However, the envisaged 1,6-elimination forming the thiohydroximate-*O*-sulfonate **25** seems to be a comparably slow process at pH 7.4 as the formation of the ITC **19** via thio-*Lossen* rearrangement is observed over 2 h. In contrast, upon addition of aqueous ammonia under basic conditions the 1,6-elimination seems to be significantly accelerated.

Similarly, also the fluorophore labelled compounds, **psGSL$_{PEG}$(NO$_2$)-DNSA** and **psGSL$_{PEG}$(NO$_2$)-BODIPY**, showed the release of their corresponding ITCs in the presence of nitroreductase (Figure 3 and 4).

When **psGSL$_{PEG}$(NO$_2$)-DNSA** (see Figure 3, A: structure, B1: R$_t$ 3.85 min and C1: mass 857 m/z for [M-K+2H]$^+$ and 777 m/z for [M-K-SO$_3$+2H]$^+$) was incubated with NfsB in the presence of FMN and NADH for 1 h at 37°C, formation of the ITC **26** (see Figure 3, A: structure, B2: R$_t$ 4.65 min and C3: mass 646 m/z for [M+Na]$^+$ and 624 m/z for [M+H]$^+$) alongside with the hydroxylamine **28** (see Figure 3, A: structure, B2: R$_t$ 3.25 min and C2: mass 842 m/z for [M-K]$^-$ and 761 m/z for [M-K-SO$_3$]$^-$) was observed. Again, addition of an excess of concentrated aqueous ammonia, rapidly converted both, ITC **26** and hydroxylamine **28** into the corresponding thiourea **27** within minutes (see Figure 3, A: structure, B3: R$_t$ = 3.32 min, and C4: mass 641 m/z for [M+H]$^+$ and 663 m/z for [M+Na]$^+$). Next, we wondered if the ITCs formed during the conversion of the *ps*GSLs may label the nitroreductase NfsB through covalent binding.

Figure 3. LC-MS analysis after incubation of **psGSL$_{PEG}$(NO$_2$)-DNSA** with nitroreductase (NTR) NfsB from *E. coli* and subsequent derivatization with NH$_4$OH solution. **A:** Structures of **psGSL$_{PEG}$(NO$_2$)-DNSA**, ITC **26**, thiourea **27** and hydroxylamine **28**. **B:** UV chromatogram at 254 nm of (B1) pure **psGSL$_{PEG}$(NO$_2$)-DNSA** (500 µM) in HEPES buffer (20 mM, pH 7.4), (B2) incubation of **psGSL$_{PEG}$(NO$_2$)-DNSA** (500 µM) with NfsB (10 µM), NADH (5 mM) and FMN (20 µM) in HEPES buffer (20mM, pH 7.4) after 1 h at 37°C and (B3) A2 and addition of aqueous NH$_4$OH solution (30 w%, 10 µL) at 23°C. **C:** ESI+ or ESI- mass analysis at (C1) 3.85 min of B1, (C2 and C3) 3.25 min and 4.65 min of B2 and (C4) 3.32 min of B3.

Scheme 4. Proposed reduction of **psGSL$_{PEG}$(NO$_2$)-N$_3$** catalyzed by the Type I oxygen-insensitive nitroreductase (NTR) NfsB from *E. coli* via ping-pong bi-bi mechanism and conversion to ITC **19**.
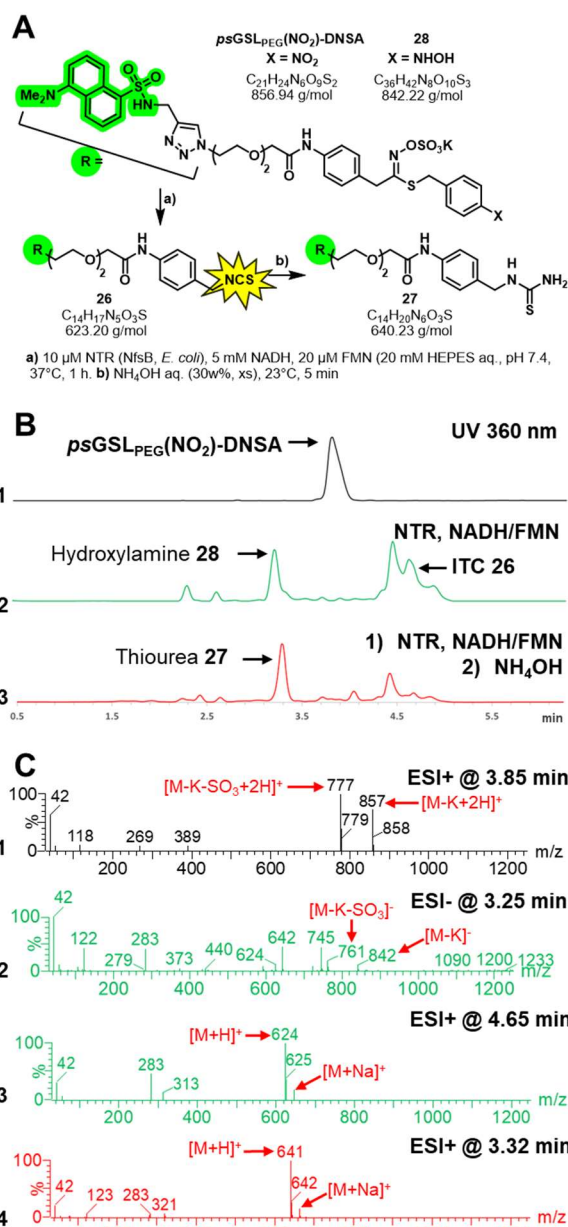
To prove this, we performed an SDS-PAGE analysis of the reaction mixtures of **psGSL$_{PEG}$(NO$_2$)-DNSA** and **psGSL$_{PEG}$(NO$_2$)-BODIPY** incubated with NfsB, FMN and NADH at 37°C for 2 h (see Figure 4, A). The gel image revealed fluorescent bands at the height of the enzyme when excited at 366 nm for both reactions, indicating a covalent labelling of NfsB (MW: 24727 Da, Uniprot P38489 with a His$_6$-tag).
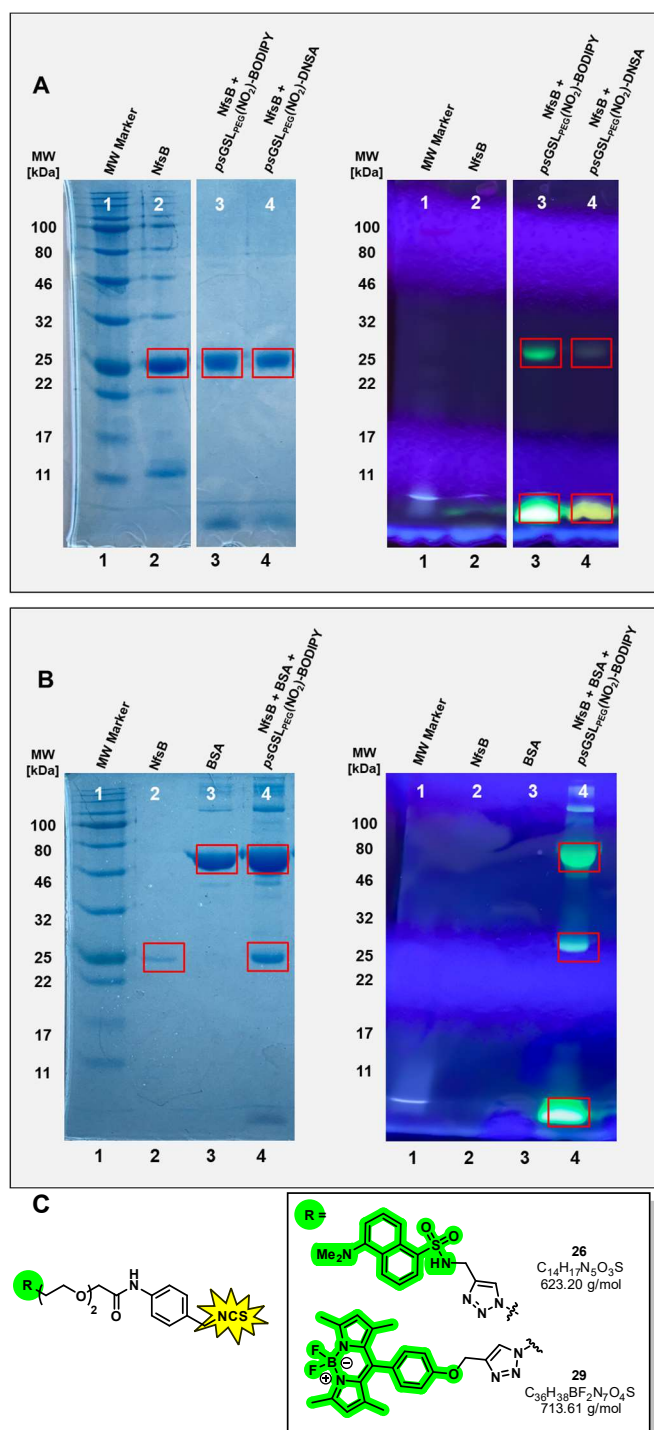
5

Figure 4. A: SDS-PAGE gel analysis of the conversion of *ps*GSL$_{PEG}$(NO$_2$)-BODIPY and *ps*GSL$_{PEG}$(NO$_2$)-DNSA in the presence of nitroreductase (NTR) NfsB from *E. coli*, left: visible light/Coomassie blue™ stain, right: UV light (366 nm), (1) molecular weight marker (3 µL, 2 mg/mL), (2) nitroreductase NfsB (10 µL, 2 mg/mL), (3) 10 µL of *ps*GSL$_{PEG}$(NO$_2$)-BODIPY (500 µM) with NfsB (10 µM), NADH (5 mM) and FMN (20 µM) in HEPES buffer (20mM, pH 7.4) after 2 h at 37°C, (4) 10 µL of *ps*GSL$_{PEG}$(NO$_2$)-DNSA (500 µM) with NfsB (10 µM), NADH (5 mM) and FMN (20 µM) in HEPES buffer (20mM, pH 7.4) after 2 h at 37°C. **B:** SDS-PAGE gel analysis of the labelling of bovine serum albumin (BSA) with *ps*GSL$_{PEG}$(NO$_2$)-BODIPY in the presence of nitroreductase (NTR) NfsB from *E. coli*, left: visible light/Coomassie blue™ stain, right: UV light (366 nm), (1) molecular weight marker (3 µL, 2 mg/mL), (2) nitroreductase NfsB (10 µL, 0.5 mg/mL), (3) BSA (10 µL, 2 mg/mL), (4) 10 µL of *ps*GSL$_{PEG}$(NO$_2$)-BODIPY (500 µM) with NfsB (10 µM), NADH (5 mM) and FMN (20 µM) in HEPES buffer (20mM, pH 7.4) and BSA (2 mg/mL) after 2 h at 37°C. **C:** Structures of ITCs **26** and **29**.

Additionally in the flow through fluorescent small molecules, presumably corresponding to the fluorescent ITCs **26** and **29** (for structures see Figure 4, C) or their hydrolysis products are visible. Furthermore, we obtained evidence for the covalent adduct by intact protein mass spectrometry. We determined a deconvoluted mass of 24726.9 Da for unmodified NfsB, which matched with the expected mass of 247267.8 Da (Uniprot P38489 with a His$_6$-tag). When *ps*GSL$_{PEG}$(NO$_2$)-N$_3$ was incubated with NfsB, FMN and NADH at 37°C for 2 h and analyzed by LC/HRMS, we were able to observe the a chromatographic peak for an NfsB variant with 964.9594 m/z with z = 26 corresponding to a that had a deconvoluted protein molecular mass of 25062.9444 Da. The mass shift of +336 Da fits well with the one expected for modification with ITC **19** (+335 Da) within the experimental error of ca. +/- 3 Da reflecting the covalent adduct mass (+336 Da) which matches the expected mass of the utilized nitroreductase NfsB (MW: 24727.8 Da, Uniprot P38489 with a His$_6$-tag) with ITC **19** (compare Figure S1 and S2 in the Supporting Information). Beyond the labelling of the converting enzyme NfsB, we could demonstrate that bovine serum albumin (BSA, 69.3 kDa, Uniprot P02769) added to the reaction mixture was also labelled efficiently with *ps*GSL$_{PEG}$(NO$_2$)-BODIPY in the presence of NfsB as show in Figure 4 B.

ITCs have been demonstrated to covalently bind peptides via irreversible formation of thioureas upon reacting with lysine residues or via reversible formation of dithiocarbamates upon reacting with cysteine residues.[56–58] While the pH optimum for the thiourea formation has been shown to be between pH 9-11, dithiocarbamates form predominately at pH 6-8.[57] Although dithiocarbamates might be the initially formed adducts, they might function as resting intermediate, reforming the ITC and finally leading to lysine thiourea adducts as stable modifications.[56]

To further elucidate how ITCs released from *ps*GSLs covalently bind to a given proteome, we next performed a chemoproteomics experiment in the proteome of *Staphylococcus aureus* SH1000 utilizing our isotopically labelled desthiobiotin-activity-based protein profiling technology (isoDTB-ABPP),[60,61] which is based on the isotopic tandem orthogonal proteolysis-ABPP (isoTOP-ABPP)[59,60] platform. Specifically, we utilized an MSFragger[61,62] based workflow that we recently established to monitor electrophile reactivity and selectivity in a completely unbiased fashion.[63]

To be compatible with the azide-containing isoDTB tags, the nitroreductase-responsive probe *ps*GSL(NO$_2$)-alkyne was synthesized from hex-5-yn-1-ol (**30**) as outlined in Scheme 5. Similar as before, the nitroreductase-responsive probe *ps*GSL(NO$_2$)-alkyne was synthesized from hex-5-yn-1-ol (**30**) as outlined in Scheme 5. Oxidation of **30** with IBX and subsequent conversion with hydroxylamine gave oxime **31** as 1:1-mixture of diastereoisomers in 67% yield.
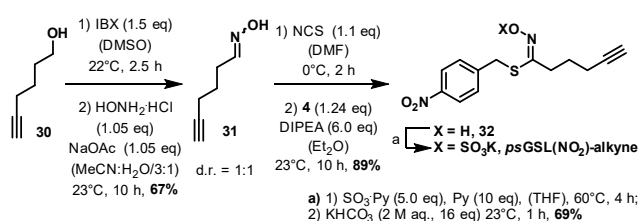
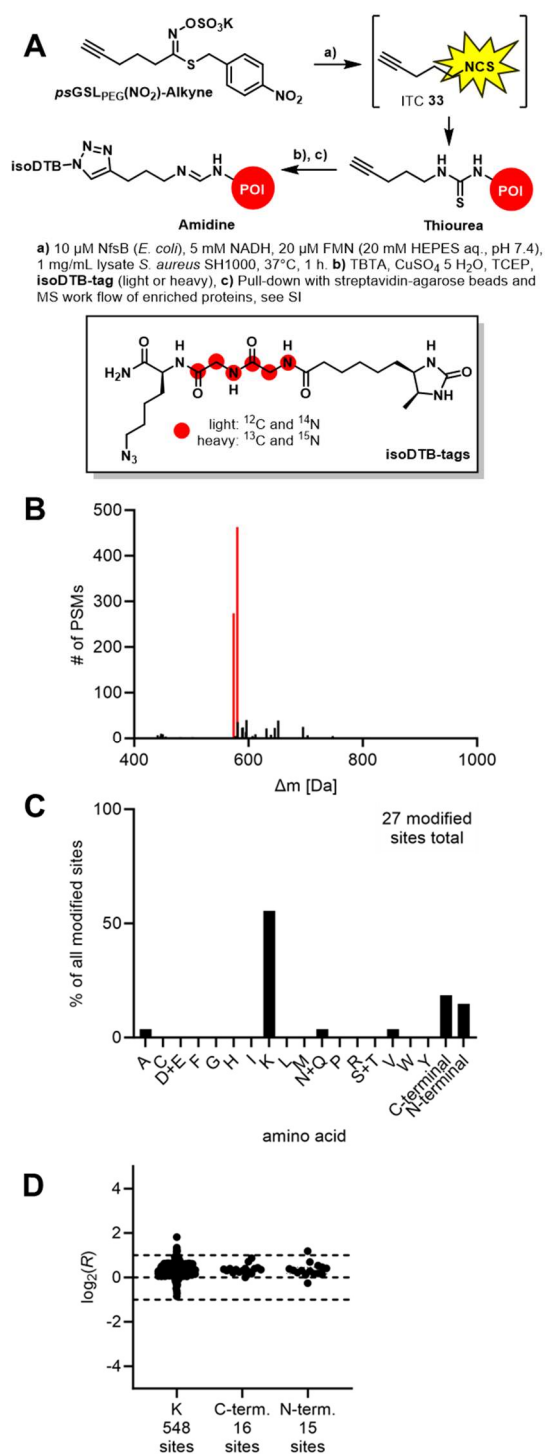**Scheme 5.** Synthesis of *ps*GSL(NO$_2$)-alkyne.

Figure 5. Labelling of *S. aureus* SH1000 proteome (at 1 mg/mL) with 100 µM of ***ps*GSL(NO₂)-alkyne** using the isoDTB-ABPP workflow[64]: **A:** Structures of ***ps*GSL(NO₂)-alkyne**, ITC **33** and the heavy and light **isoDTB-tags**; general structures of thioureas and isoDTB-tag-clicked amidines (POI = protein of interest). **B:** Masses of modification determined through analysis with an Open Search in MSFragger[61,62] **C:** Amino acid selectivity determined through an Offset Search that localizes the modification to the modified amino acid(s) In this way, selectivity is assessed across all proteinogenic amino acids. The bar represents the fraction of all modified sites that is modified at the indicated amino acid. **D:** Quantification of the modification at the main amino acid residues identified in the offset search at the selected masses was performed using a Closed Search and the IonQuant[65] feature. The heavy and light samples were mixed at a ratio of 1:1. The dashed lines indicate the expected values of log2(R) = 0 and the preferred window of quantification (−1 < log2(R) < 1). All data is based on technical duplicates.

Formation of the chloro oxime and subsequent coupling with para-nitrobenzylthiol (**4**) gave the thiohydroximate **32**, which was treated with pyridine SO₃ complex and potassium hydrogen carbonate solution to obtain ***ps*GSL(NO₂)-alkyne**.

With ***ps*GSL(NO₂)-alkyne** in hand, two identical samples of freshly prepared lysate of *S. aureus* SH1000 were incubated with the probe in presence of nitroreductase NfsB from *E. coli*, FMN and NADH for 1 h at 37°C (see Figure 5, A) to form protein adducts.

In one sample the heavy **isoDTB-tag** was attached to the terminal alkyne via CuAAC and in the other one the corresponding light **isoDTB-tag**. Afterwards the samples were combined and a pull-down of isoDTB-labelled proteins utilizing streptavidin-agarose beads was performed. The enriched protein fractions were digested, subjected to a streamlined mass sample preparation and the modified peptides were analyzed by LC-MS/MS.

Surprisingly, the almost exclusively observed proteome modification was found to be an amidine instead of the expected thiourea obtained in the other experiments performed (Figure 5B). Currently, we believe that a substrate-dependent, acid-catalyzed desulfurization is occurring in presence of TFA during the sample preparation of the isoDTB-ABPP workflow or during ionization in the LCMS. Oxidative formation of amidines from thioureas is known in the presence of strong oxidants such as hydrogen peroxide under acidic conditions already at 25°C.[66] Attempts to facilitate amidine formation under similar conditions led to formation of only traces of corresponding amidines in presence of formic acid or TFA at 23°C. (See Figure S3 in the Supporting Information). The exact mechanism and nature of this desulfurization is still under investigation. However, according to the isoDTB-ABPP workflow this is the main modification that is detected by chemoproteomic analysis.

We next used the mass of modification of amidine formation as input for an offset search to study the amino acid selectivity (Figure 5C).[63] The modification was mainly localized to amino groups in the detected proteins (lysines and protein *N*-termini) as expected with some surprising reactivity also at protein *C*-termini. Overall, the modification does not seem to be very stable under the detection conditions as seen by the low number of localized sites after the application of the very stringent filters of the offset search (27 sites unambiguously localized). This indicates that the modification is easily lost upon fragmentation in the mass spectrometer. As discussed above, modification of cysteines with ITCs is expected to be reversible, explaining why cysteine modification cannot be detected in this experiment. Overall, the amidine modification of the proteome mainly localized to lysines and the protein termini.

In the final stage of the isoDTB-ABPP analysis, we quantified the residues that are modified with the amidine modification. It is striking, that under the less stringent localization filters used for quantification, we mainly identify lysine modification indicating that stability of the modification at lysines is the main limitation to high quality localization and that the probe actually mainly leads to lysine-modified peptides. Of the 548 modified lysine sites, the vast majority was quantified with a small spread around the expected log2(R) of 0 indicating reliable quantification of these modified peptides. Among the 548 modified lysines were 265 that were identified in 89 different essential proteins. These include lysines in important functional sites of the proteins such as those forming Schiff Bases during catalysis (K82 of pyridoxal 5'-phosphate synthase pdxS and K151 of deoxyribose-phosphate

7

aldolase deoC), other residues at active sites (K596 of glutamine-fructose-6-phosphate aminotransferase glmS and K217 of ribitol-5-phosphate cytidylyltransferase 1 tarI), residues at nucleotide binding sites (K71 at the ATP binding site of formate-tetrahydrofolate ligase fhs, K23 at the GTP binding site of elongation factor G fusA and K46 of the ATP binding site of succinate-CoA ligase sucC) and, strikingly, at DNA binding sites of transcriptional regulators (K52 and K56 of HTH-type transcriptional regulator SarR and K57 and K74 of HTH-type transcriptional regulator MgrA). While the performed isoDTB-ABPP experiment does not inform on the stoichiometry of engagement at these residues, it is a good indication that ITCs can exert an effect in bacteria through engagement of a variety of functional lysines in proteins.

Conclusion

Here, we have introduced the concept of *pseudo*glucosinolates (*ps*GSLs) that can be activated into isothiocyananates (ITCs) with non-canonical enzymes. We have demonstrated the release of ITCs from **$psGSL_{PEG}(NO_2)$-N$_3$**, **$psGSL_{PEG}(NO_2)$-BODIPY**, **$psGSL_{PEG}(NO_2)$-DNSA** and **$psGSL(NO_2)$-alkyne** in the presence of nitroreductase NfsB from *E. coli*. The released ITCs were demonstrated to be effective in labelling of BSA and show a predominantly lysine-selective modification of proteins in the entire proteome including at many functional sites of essential proteins. In contrast to natural GSLs, *ps*GSLs represent a complementary prodrug approach for bio-responsive release of ITCs, which hold potential to be adjusted in their bio-responsiveness towards multiple enzymes and chemical microenvironments. The concept of *ps*GSLs might find application in chemical biology for enzyme-dependent labelling of biomolecules and prodrug approaches to exploit the broad variety of interesting biological activities of potentially hydrolysis sensitive ITCs.[20]

Currently, the protection of the *para*-aminobenzylthiol unit with different peptidase-, oxidoreductase- and hydrolases-responsive masking groups is under investigation to expand the concept of *ps*GSLs towards a platform technology for bio-responsive protein labelling and ITC-based covalent inhibitors of proteins.

Supporting Information

The authors have cited additional references within the Supporting Information.[61–65,67,68,68–77]

Acknowledgements

Author contributions

The research was conceived by PK. The manuscript was written by PK with contributions from CSGG, AS, MDK, MZ, SAS, MB and SMH. The SI was written by PK, CCJ, LW, CSGG, MDK, AC, MZ, and UB. All compounds were synthesized by CCJ, LW, AC and MDK. Biochemical evaluation of all compounds in the presence of enzymes were planned by PK and CCJ, CSGG and conducted by CCJ and CSGG. HRMS analysis of labelled proteins and enzymes were planned by PK, MB and conducted by UB and CCJ. Analysis of labelled proteins via gel electrophoresis was planned by PK, CCJ and CSGG and conducted by CCJ and CSGG. MS-MS analysis of labelled *S. aureus* proteome was planned by SMH, SAS and MZ and conducted by MZ. All authors have given approval to the final version of the manuscript.

[1] F. S. Hanschen, E. Lamy, M. Schreiner, S. Rohn, *Angew. Chem. Int. Ed.* **2014**, *53*, 11430–11450.

[2] A. M. Bones, J. T. Rossiter, *Phytochemistry* **2006**, *67*, 1053–1067.

[3] I. Winde, U. Wittstock, *Phytochemistry* **2011**, *72*, 1566–1575.

[4] K. G. Ramawat, J.-M. Mérillon, Eds. , *Glucosinolates*, Springer, **2017**.

[5] S. D. Johnson, M. E. Griffiths, C. I. Peter, M. J. Lawes, *Am. J. Bot.* **2009**, *96*, 2080–2086.

[6] L. Romeo, R. Iori, P. Rollin, P. Bramanti, E. Mazzon, J. W. Fahey, A. T. Zalcmann, P. Talalay, *Molecules* **2018**, *23*, 624.

[7] M. G. Kim, H. S. Lee, *J. Food Sci.* **2009**, *74*, 467–471.

[8] L. Ugolini, G. Cilia, E. Pagnotta, L. Malaguti, V. Capano, I. Guerra, L. Zavatta, S. Albertazzi, R. Matteo, L. Lazzeri, L. Righetti, A. Nanetti, *Biomolecules* **2021**, *11*, 1657.

[9] A. Nanetti, L. Ugolini, G. Cilia, E. Pagnotta, L. Malaguti, I. Cardaio, R. Matteo, L. Lazzeri, *Microorganisms* **2021**, *9*, 949.

[10] C. Dias, A. Aires, M. Saavedra, *Int. J. Mol. Sci.* **2014**, *15*, 19552–19561.

[11] D. Nowicki, O. Rodzik, A. Herman-Antosiewicz, A. Szalewska-Pałasz, *Sci. Rep.* **2016**, *6*, 22263.

[12] S. J. Kaiser, N. T. Mutters, B. Blessing, F. Günther, *Fitoterapia* **2017**, *119*, 57–63.

[13] C. Melim, M. R. Lauro, I. M. Pires, P. J. Oliveira, C. Cabral, *Pharmaceutics* **2022**, *14*, 190.

[14] J. Melrose, *Biomedicines* **2019**, *7*, 62.

[15] E. L. Connolly, M. Sim, N. Travica, W. Marx, G. Beasy, G. S. Lynch, C. P. Bondonno, J. R. Lewis, J. M. Hodgson, L. C. Blekkenhorst, *Front. Pharmacol.* **2021**, *12*, Article 767975.

[16] P. Soundararajan, J. Kim, *Molecules* **2018**, *23*, 2983.

[17] Q. V. Vo, C. Trenerry, S. Rochfort, J. Wadeson, C. Leyton, A. B. Hughes, *Bioorg. Med. Chem.* **2013**, *21*, 5945–5954.

[18] N. Orouji, S. K. Asl, Z. Taghipour, S. Habtemariam, S. M. Nabavi, R. Rahimi, *Med. Oncol.* **2023**, *40*, 344.

[19] Ł. Janczewski, *Molecules* **2022**, *27*, 1750.

[20] X. Tian, J. Gao, M. Liu, Y. Lei, F. Wang, J. Chen, P. Chu, J. Gao, F. Long, M. Liang, X. Long, H. Chu, C. Liu, X. Li, Q. Sun, G. Li, Y. Yang, *J. Med. Chem.* **2020**, *63*, 3881–3895.

[21] A. Narbad, J. T. Rossiter, *Mol. Nutr. Food Res.* **2018**, *62*, 1–10.

[22] C. S. Liou, S. J. Sirk, C. A. C. Diaz, A. P. Klein, C. R. Fischer, S. K. Higginbottom, A. Erez, M. S. Donia, J. L. Sonnenburg, E. S. Sattely, *Cell* **2020**, *180*, 717-728.e19.

[23] V. Luang-In, A. A. Albaser, C. Nueno-Palop, M. H. Bennett, A. Narbad, J. T. Rossiter, *Curr. Microbiol.* **2016**, *73*, 442–451.

[24] D. Cerniauskaite, J. Rousseau, A. Sackus, P. Rollin, A. Tatibouët, *Eur. J. Org. Chem.* **2011**, 2293–2300.

[25] W. Abramski, M. Chmielewski, *J. Carbohydr. Chem.* **2006**, *15*, 109–113.

[26] M. S. C. Pedras, Q. H. To, G. Schatte, *Chem. Commun.* **2016**, *52*, 2505–2508.

[27] M. Mavratzotis, S. Cassel, S. Montaut, P. Rollin, *Molecules* **2018**, *23*, 1–15.

[28] Y. W. Lim, M. J. H. Ong, R. J. Hewitt, *Synthesis* **2018**, *50*, 1640–1650.

[29] J. J. Morrison, N. P. Botting, A. A. B. Robertson, *J Label Compd Radiopharm* **2007**, *50*, 260–263.

[30] N. P. Botting, A. A. B. Robertson, J. J. Morrison, *J. Label. Compd. Radiopharm.* **2007**, *50*, 260–263.

[31] J. T. Rossiter, J. A. Pickett, M. H. Bennett, A. M. Bones, G. Powell, J. Cobb, *Phytochemistry* **2007**, *68*, 1384–1390.

[32] M. S. C. Pedras, Q. H. To, *J. Label. Compd. Radiopharm.* **2018**, *61*, 94–106.

[33] Q. Zhang, T. Lebl, A. Kulczynska, N. P. Botting, *Tetrahedron* **2009**, *65*, 4871–4876.

[34] M. Blanc-Muesser, H. Driguez, B. Joseph, M. C. Viaud, P. Rollin, *Tetrahedron Lett.* **1990**, 3867–3868.

[35] Q. V. Vo, S. Rochfort, P. C. Nam, T. L. Nguyen, T. T. Nguyen, A. Mechler, *Carbohydr. Res.* **2018**, *455*, 45–53.

[36] G. Cutolo, F. Reise, M. Schuler, R. Nehmé, G. Despras, J. Brekalo, P. Morin, P.-Y. Renard, T. K. Lindhorst, A. Tatibouët, *Org. Biomol. Chem.* **2018**, *16*, 4900–4913.

[37] G. Cutolo, B. Didak, J. Tomas, B. Roubinet, P. Lafite, R. Nehmé, M. Schuler, L. Landemarre, A. Tatibouët, *Carbohydr. Res.* **2022**, *516*, 108562.

[38] C. P. Glindemann, A. Backenköhler, M. Strieker, U. Wittstock, P. Klahn, *ChemBioChem* **2019**, *19*, 1668–1694.

[39] C. Sabot, J. W. Fredy, G. Cutolo, B. Poret, R. Nehmé, M. Hubert-Roux, P. Gandolfo, H. Castel, M. Schuler, A. Tatibouët, P.-Y. Renard, *Bioconjug. Chem.* **2019**, *30*, 1385–1394.

[40] C. Kanstrup, C. C. Jimidar, J. Tomas, G. Cutolo, C. Crocoll, M. Schuler, P. Klahn, A. Tatibouët, H. H. Nour-Eldin, *Int. J. Mol. Sci.* **2023**, *24*, 920.

[41] J. Zhang, X. Li, P. Ge, B. Zhang, L. Wen, C. Gu, X. Zhou, *Sep. Purif. Rev.* **2022**, *51*, 330–339.

[42] G. Tian, P. Tang, R. Xie, L. Cheng, Q. Yuan, J. Hu, *Food Chem.* **2016**, *199*, 301–306.

[43] C. C. Jimidar, J. Grunenberg, B. Karge, H. L. S. Fuchs, M. Brönstrup, P. Klahn, *Chem. – A Eur. J.* **2022**, *28*, e202103525.

[44] O. A. Okoh, P. Klahn, *ChemBioChem* **2018**, *19*, 1668–1694.

[45] P. Klahn, V. Fetz, A. Ritter, W. Collisi, B. Hinkelmann, T. Arnold, W. Tegge, K. Rox, S. Hüttel, K. I. K. I. K. I. Mohr, J. Wink, M. Stadler, J. Wissing, L. Jänsch, M. Brönstrup, *Chem. Sci.* **2019**, *10*, 5197–5210.

[46] Y. Bourgat, C. Mikolai, M. Stiesch, P. Klahn, H. Menzel, *Antibiotics* **2021**, *10*, 653.

[47] R. Zscherp, J. Coetzee, J. Vornweg, J. Grunenberg, J. Herrmann, R. Müller, P. Klahn, *Chem. Sci.* **2021**, *12*, 10179–10190.

[48] C. C. Jimidar, L. Wiese, M. Stirz, U. Beutling, A. Schallmey, M. Brönstrup, P. Klahn, in *Poster 34. Irseer Naturstofftage*, **2022**.

[49] P. Rollin, A. Tatibouët, *Comptes Rendus Chim.* **2011**, *14*, 194–210.

[50] S. Zenno, H. Koike, M. Tanokura, K. Saigo, *J. Biochem.* **1996**, *120*, 736–744.

[51] F. J. Peterson, R. P. Mason, J. Hovsepian, J. L. Holtzman, *J. Biol. Chem.* **1979**, *254*, 4009–4014.

[52] A. Christofferson, J. Wilkie, *Biochem. Soc. Trans.* **2009**, *37*, 413–418.

[53] P. R. Race, A. L. Lovering, R. M. Green, A. Ossor, S. A. White, P. F. Searle, C. J. Wrighton, E. I. Hyde, *J. Biol. Chem.* **2005**, *280*, 13256–13264.

[54] M. W. Mullowney, N. I. Maltseva, E. Endres, Y. Kim, A. Joachimiak, T. S. Crofts, *Microbiol. Spectr.* **2022**, *10*, e00139-22.

[55] T. S. Crofts, P. Sontha, A. O. King, B. Wang, B. A. Biddy, N. Zanolli, J. Gaumnitz, G. Dantas, *Cell Chem. Biol.* **2019**, *26*, 559-570.e6.

[56] T. Nakamura, Y. Kawai, N. Kitamoto, T. Osawa, Y. Kato, *Chem. Res. Toxicol.* **2009**, *22*, 536–542.

[57] L. Petri, P. A. Szijj, Á. Kelemen, T. Imre, Á. Gömöry, M. T. W. Lee, K. Hegedűs, P. Ábrányi-Balogh, V. Chudasama, G. M. Keserű, *RSC Adv.* **2020**, *10*, 14928–14936.

[58] I. Karlsson, K. Samuelsson, D. J. Ponting, M. Törnqvist, L. L. Ilag, U. Nilsson, *Sci. Rep.* **2016**, *6*, 21203.

[59] K. M. Backus, B. E. Correia, K. M. Lum, S. Forli, B. D. Horning, G. E. González-Páez, S. Chatterjee, B. R. Lanning, J. R. Teijaro, A. J. Olson, D. W. Wolan, B. F. Cravatt, *Nature* **2016**, *534*, 570–574.

[60] E. Weerapana, C. Wang, G. M. Simon, F. Richter, S. Khare, M. B. D. Dillon, D. A. Bachovchin, K. Mowen, D. Baker, B. F. Cravatt, *Nature* **2010**, *468*, 790–795.

[61] A. T. Kong, F. V Leprevost, D. M. Avtonomov, D. Mellacheruvu, A. I. Nesvizhskii, *Nat. Methods* **2017**, *14*, 513–520.

[62] F. Yu, G. C. Teo, A. T. Kong, S. E. Haynes, D. M. Avtonomov, D. J. Geiszler, A. I. Nesvizhskii, *Nat. Commun.* **2020**, *11*, 4065.

[63] P. R. A. Zanon, F. Yu, P. Z. Musacchio, L. Lewald, M. Zollo, K. Krauskopf, D. Mrdovic, P. Raunft, T. E. Maher, M. Cigler, C. J. Chang, K. Lang, F. D. Toste, A. I. Nesvihskii, S. M. Hacker, D. Mrdović, P. Raunft, T. E. Maher, M. Cigler, C. J. Chang, K. Lang, F. D. Toste, A. I. Nesvizhskii, S. M. Hacker, *ChemRxiv* **2021**, *1*, DOI: 10.26434/chemrxiv-2021-w7rss-v2.

[64] P. R. A. Zanon, L. Lewald, S. M. Hacker, *Angew. Chem. Int. Ed.* **2020**, *59*, 2829–2836.

[65] F. Yu, S. E. Haynes, G. C. Teo, D. M. Avtonomov, D. A. Polasky, A. I. Nesvizhskii, *Mol. Cell. Proteomics* **2020**, *19*, 1575–1585.

[66] S. Grivas, E. Ronne, L. Vares, I. Kühn, A. Claesson, J. Arnarp, L. Björk, R. Gawinecki, *Acta Chem. Scand.* **1995**, *49*, 225–229.

[67] G. Clavé, H. Boutal, A. Hoang, F. Perraut, H. Volland, P. Y. Renard, A. Romieu, *Org. Biomol. Chem.* **2008**, *6*, 3065–3078.

[68] A. J. O'Neill, *Lett. Appl. Microbiol.* **2010**, *51*, 358–361.

[69] T. Rizk, E. J.-F. Bilodeau, A. M. Beauchemin, *Angew. Chem. Int. Ed.* **2009**, *48*, 8325–8327.

[70] M. J. Horsburgh, J. L. Aish, I. J. White, L. Shaw, J. K. Lithgow, S. J. Foster, *J. Bacteriol.* **2002**, *184*, 5457–5467.

[71] D. Kessner, M. Chambers, R. Burke, D. Agus, P. Mallick, *Bioinformatics*

9

2008, *24*, 2534–2536.

[72] F. da Veiga Leprevost, S. E. Haynes, D. M. Avtonomov, H.-Y. Chang, A. K. Shanmugam, D. Mellacheruvu, A. T. Kong, A. I. Nesvizhskii, *Nat. Methods* **2020**, *17*, 869–870.

[73] M. Frigerio, M. Santagostino, S. Sputore, *J. Org. Chem.* **1999**, *64*, 4537–4538.

[74] Y. Nishio, R. Mifune, T. Sato, S. Ishikawa, H. Matsubara, *Tetrahedron Lett.* **2017**, *58*, 1190–1193.

[75] J. R. Guo, H. Y. Huang, Y. L. Yan, C. F. Liang, *Asian J. Org. Chem.* **2018**, *7*, 179–188.

[76] N. Dubey, P. Sharma, A. Kumar, *Synth. Commun.* **2015**, *45*, 2608–2626.

[77] M. Rauschenberg, E. C. Fritz, C. Schulz, T. Kaufmann, B. J. Ravoo, *Beilstein J. Org. Chem.* **2014**, *10*, 1354–1364.